All-Optical Switching Improvement Using Photonic-Crystal Fano Structures

Yu, Yi; Xue, Weiqi; Hu, Hao; Oxenløwe, Leif Katsuo; Yvind, Kresten; Mørk, Jesper

Published in:
IEEE Photonics Journal

Link to article, DOI:
10.1109/JPHOT.2016.2523244

Publication date:
2016

Document Version
Publisher's PDF, also known as Version of record

IEEE Photonics Journal
An IEEE Photonics Society Publication

Open Access

All-Optical Switching Improvement Using Photonic-Crystal Fano Structures

Volume 8, Number 1, February 2016

Yi Yu
Weiqi Xue
Hao Hu
Leif Katsuo Oxenløwe
Kresten Yvind
Jesper Mork

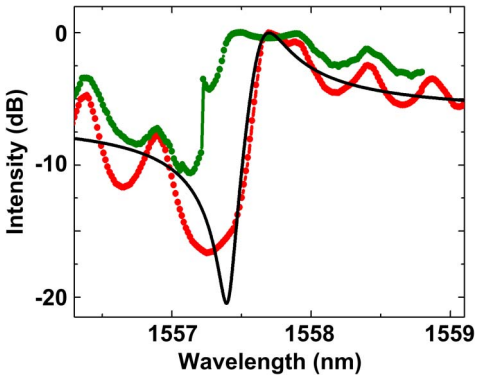

DOI: 10.1109/JPHOT.2016.2523244
1943-0655

IEEE photonics SOCIETY
IEEE

All-Optical Switching Improvement Using Photonic-Crystal Fano Structures

Yi Yu, Weiqi Xue, Hao Hu, Leif Katsuo Oxenløwe, Kresten Yvind, and Jesper Mork

DTU Fotonik, Department of Photonics Engineering, Technical University of Denmark, DK-2800 Kongens Lyngby, Denmark

DOI: 10.1109/JPHOT.2016.2523244

Manuscript received December 8, 2015; revised January 19, 2016; accepted January 25, 2016. Date of publication January 28, 2016; date of current version April 15, 2016. This work was supported by the Villum Fonden through the NAnophotonics for TErabit Communications (NATEC) Centre. Corresponding author: Y. Yu (e-mail: yiyu@fotonik.dtu.dk).

Abstract: We investigate the intensity and phase response of optical switches based on a photonic crystal waveguide coupled to a nanocavity. In particular, we compare the performances of switches with traditional Lorentzian transmission spectrum to switches displaying an asymmetric Fano shape, as obtained by incorporating a partially transmitting element in the waveguide. Compared to traditional Lorentzian structures, the Fano structure shows improved switching contrast and speed without adding any extra phase modulation, corresponding to a much lower chirp parameter. Using a simple and ultra-compact InP photonic-crystal Fano structure with broken mirror symmetry, we experimentally demonstrate 20-Gb/s all-optical switching with low-energy consumption.

Index Terms: Nonlinear optical devices, photonic crystals, Fano resonance, all-optical devices.

1. Introduction

High-speed, low-energy photonic switches that can be integrated with waveguides and other functional devices may become key elements in realizing next-generation integrated optical circuits that can meet the growing demand for information capacity [1], [2]. In resonator based switches, the transmission of the data signal can be controlled by shifting the cavity resonance via an optical control signal [3], [4]. The energy consumption of the device is highly dependent on the shape of the transmission spectrum which determines the refractive index shift required for achieving a certain on-to-off ratio [3], [5], [6]. As shown in Fig. 1(a), the extended tails of a Lorentzian spectrum imply large switching energies, since the resonance needs to be shifted significantly (as the horizontal black arrow indicates) to properly switch the signal. In contrast, a Fano resonance [7] may show an asymmetric spectrum, featuring a large transmission change within a narrow wavelength range (as illustrated by the horizontal green arrow), determined by the transition from constructive to destructive interference between the discrete resonance and the continuum, thus enabling low-energy switching. The advantage of a Fano resonance was demonstrated using a symmetric photonic-crystal (PhC) structure [8], and it was also found that the non-monotonous frequency-dependence of the tail of the Fano transfer function implies an inherent reduction of patterning effects. In contrast, a Lorentzian spectrum has

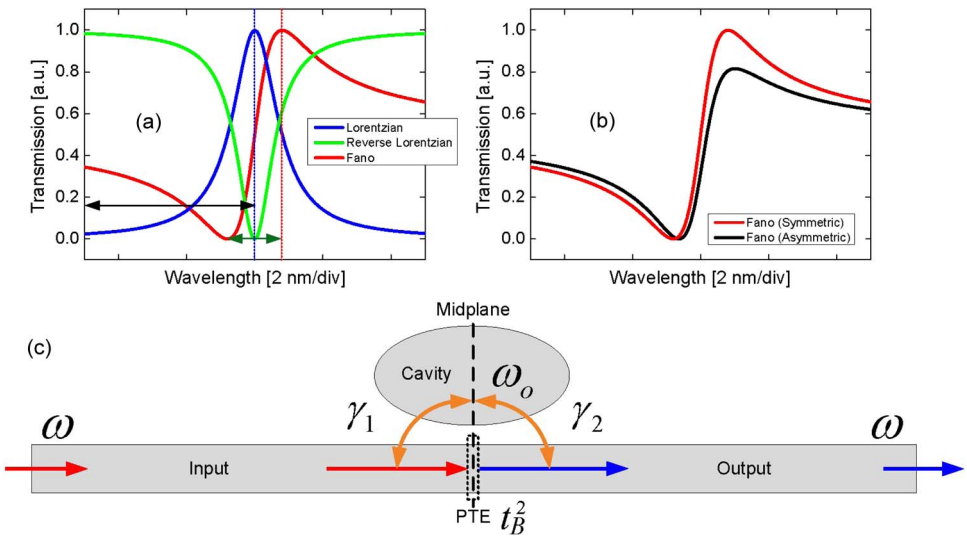

Fig. 1. (a) Comparison of transmission spectra for structures with Lorentzian and Fano-type resonances. The Q-factors and resonance wavelengths are the same. (b) Transmission spectra for Fano resonance with and without mirror symmetry. (c) Transmission of a signal at frequency ω through a waveguide that is side-coupled to a cavity with resonance frequency ω_0. The field in the cavity couples to the in- and output ports with decay rates γ_1 and γ_2. A partially transmitting element (PTE, dashed rectangle) with power transmission t_B^2 is placed at the mid-plane.

monotonously-varying tails which convert the (slow) dynamics of the resonance shift into amplitude modulation, limiting the bitrate due to the long carrier lifetime [8]–[10].

In this paper, we present a detailed experimental and theoretical comparison of the switching performances of Lorentzian and Fano cavity-waveguide structures realized in InP photonic-crystal membranes. In [11] and [12], we presented the first results of such a comparison but here we extend the theoretical analysis of the switching performance, as well as presenting experimental and theoretical results on the intensity and phase response. It is found that the chirp-parameter of a Fano resonance may be reduced compared to that of a traditional Lorentzian resonance. The bit error rate (BER) performance of different switching configurations is compared, and it is shown that an ultra-compact Fano structure with broken mirror symmetry allows experimental demonstration of 20 Gbit/s all-optical switching with low-energy consumption.

2. Comparison of Lorentzian and Fano Structures

The investigated structure (see Fig. 1(c)) consists of a line-defect waveguide coupled to a point-defect nanocavity [13]. In contrast to an ordinary side-coupled system [14], we add below the nanocavity a partially transmitting element (PTE) that allows controlling the amplitude of the continuum-path. This PTE can be realized by a blockade hole (BH), with a transmission coefficient t_B that can be varied via the radius R_B of the BH [12], [13]. By tuning t_B between 0 to 1 through adjusting R_B, the transmission spectrum of the structure can be varied between a symmetric Lorentzian shape and an asymmetric Fano shape. The PTE also causes additional vertical scattering loss, but from simulations this loss is found to be insignificant and is neglected in the theoretical simulations.

The dynamical properties of the waveguide-cavity structures can be analyzed using nonlinear temporal coupled mode theory [15], [16]. First, we numerically investigate the high-speed all-optical switching performance of comparable Fano and Lorentzian structures using a pseudo-random binary sequence (PRBS) for the pump signals; cf. Fig. 2. When the probe signal is initially blue detuned and a strong pump pulse is injected into the cavity, free carriers are generated by two-photon absorption, causing strong carrier-induced nonlinearity which dominates over the Kerr and thermo-optic effect, shifting the cavity resonance towards shorter

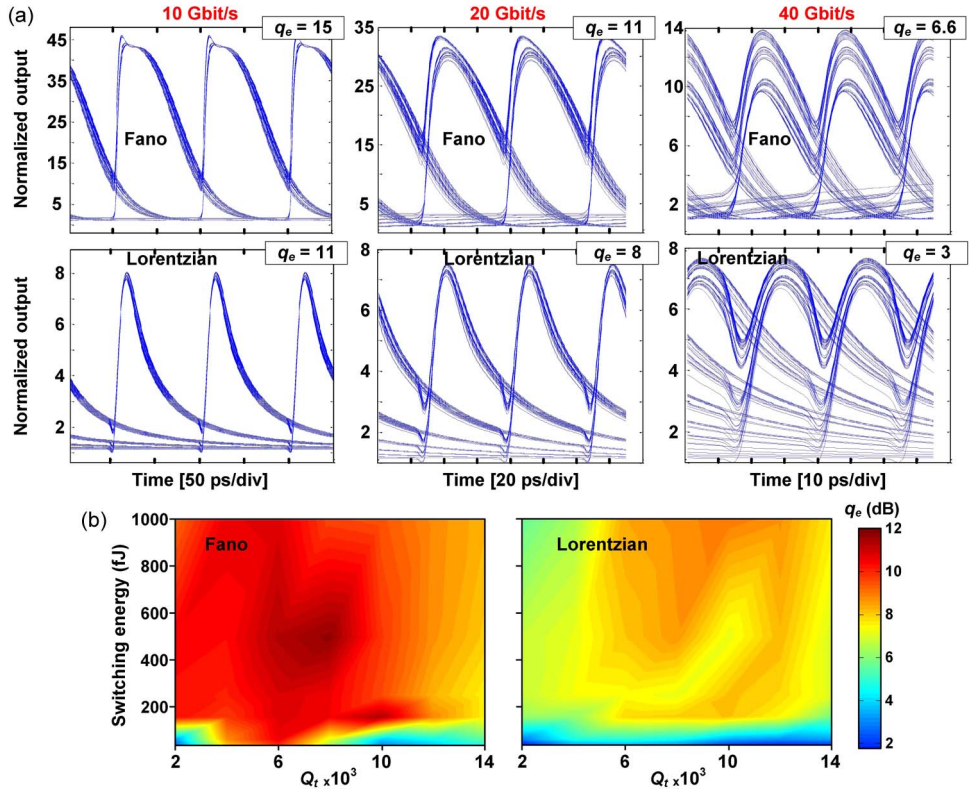

Fig. 2. (a) Calculated eye diagrams of the converted signal for comparable Lorentzian and Fano structures with the same Q-factor at 10, 20, and 40 Gbit/s. The outputs have been normalized to their minimum values. The extracted values of the quality factor q_e (in dB) of the eye diagram are given in the figures. The total Q-factor Q_t is 4000, and the intrinsic Q-factor Q_v is 12000. The pump pulse has a Gaussian shape with a full-width at half-maximum of 5 ps and a pulse energy of 164 fJ/bit. (b) Contour plots of the largest achievable value of q_e at 40 Gbit/s upon variation of total Q-factor Q_t and pump energy for the Fano (left) and Lorentzian (right) structure. The intrinsic Q-factor of the two structures is infinite.

wavelengths, hence increasing the probe transmission. It is seen that the Fano structure has a considerably larger eye opening than the Lorentzian structure, which is ascribed to the suppression of the slow decay component of the signal amplitude variation. We quantify the performance by calculating a quality factor q_e from the eye diagram, defined as the maximum value of $(P_1 - P_0)/(\sigma_1 + \sigma_0)$ achieved within one period, where P_1 and P_0 are the average output powers corresponding to "1" and "0" levels, respectively, at each sampling time, and σ_1 and σ_0 are the corresponding standard deviations. Notice that the bit-error rate cannot be inferred from the value of q_e since the widths of the 0 and 1 bit distributions arise from deterministic patterning effects rather than random noise leading to Gaussian distributions. Nevertheless, q_e is a measure of the distortion of the eye due to patterning effects. Since no obvious overshoots are found in the eye diagrams, a smaller value will, in combination with random receiver noise, e.g., lead to higher bit-error rate. In Fig. 2, for each pair of values of the cavity quality factor Q_t and pump energy, the largest q_e is found by scanning the signal detuning. For both the Fano and Lorentzian structure, the maximum value of q_e is obtained for moderate Q_t, since a higher quality factor will degrade the signal due to a longer photon lifetime. The Fano structure is seen to result in a better q_e than the Lorentzian structure over a wide range of cavity quality factors, achieving eye quality factors q_e of up to 12 dB, which could not be achieved using a Lorentzian structure. Simulations for other values of the transmittance, t_B^2, show that the advantage of Fano over Lorentzian structures is a common feature.

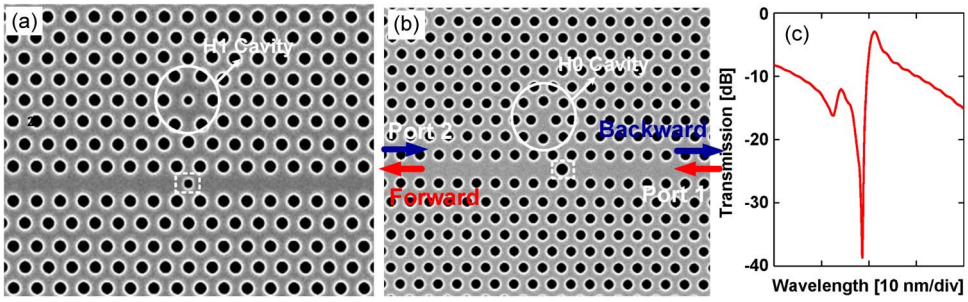

Fig. 3. (a) Fabricated InP membrane structure. (a) Symmetric Fano structure with an H1 nanocavity. (b) Fano structure with an H0 nanocavity is made asymmetric with respect to the mid-plane by displacing the blocking hole (BH) by one lattice constant towards port 1. (c) FDTD-simulated transmission spectrum of the asymmetric Fano structure.

Fig. 3(a) shows an example of the fabricated PhC InP membrane. An H1 nanocavity is side-coupled to a standard W1-defect type waveguide. The device is equipped with mode adapters to facilitate out coupling [17]. The detailed fabrication processes were described in [18]. In general, when a signal is transmitted through a switch (or modulator), not only the intensity but also the phase of the signal is modified, as quantified by the chirp-parameter giving the ratio of phase and amplitude changes [19]. We measured the transmission phase response of the structure by comparing the microwave phase shift of the modulated envelope of the signal before and after the structure [20]. A CW light beam from a tunable laser source was modulated at 10 GHz using a dual drive Mach–Zehnder modulator driven by a microwave signal from a network analyzer, so that the generated signal is single-sideband. The input signal was set to TE polarization using a polarizer and fed into the device. The output of the device under test was sent to an InGaAs photodetector with a bandwidth of 50 GHz, converting the signal back to the electrical domain, and measured by the network analyzer (scattering parameter S21), through which the microwave phase shift $\Delta\phi_{NA}(\omega)$ was obtained. By sweeping the input light from shorter to longer wavelengths across the resonance, we obtain the group delay of the system $\tau_g(\omega) = -\partial\phi(\omega)/\partial\omega = \Delta\phi_{NA}(\omega)/(2\pi f_m)$, where $f_m = 10$ GHz. The corresponding phase response $\phi(\omega)$ can be obtained by integration. In order to remove the phase shift contribution of the setup itself (i.e., fibers, couplers, amplifiers, etc.), the linear part of the phase response (delay) was estimated by characterizing a PhC reference waveguide (without cavity and PTE), resulting in the reference characteristic, $\phi_r(\omega)$. The phase shift originating from the cavity resonance was then obtained as $\phi_c(\omega) = \phi(\omega) - \phi_r(\omega)$. During the measurements, an erbium-doped optical fiber amplifier (EDFA) and a variable optical attenuator were included at the input of the structure to tune the input optical power level.

Fig. 4 shows the measured intensity and corresponding phase spectra of a Fano and Lorentzian structure [8]. We see that for sufficiently low input power, the measured spectra agree very well with linear theory. For higher input power, the abrupt changes of output power with wavelength occur due to the existence of a spectral region of bistability located on the blue side of the resonance. Since the tunable laser was scanned from shorter to longer wavelengths, the transmission normally follows the lower branch of the bistability curve. From Fig. 4, we find that since the Fano resonance reflects an interference between a traditional Lorentzian resonance and a continuum mode, so that both destructive and instructive interference occur within the resonance bandwidth. This gives a local maximum and minimum within the bandwidth of the Lorentzian transfer function, thus enhancing the transmission variation (contrast) between the maximum and minimum for the Fano resonance, while the largest phase change is kept almost the same. In this case, a small nonlinear blueshift of the Fano resonance imposes a larger intensity change than for a Lorentzian, while the phase shifts are similar. These results suggest that Fano structures are promising for realizing intensity modulators with large modulation contrast and small chirp-parameter. Since the chirp-parameter is time dependent, it is not instructive

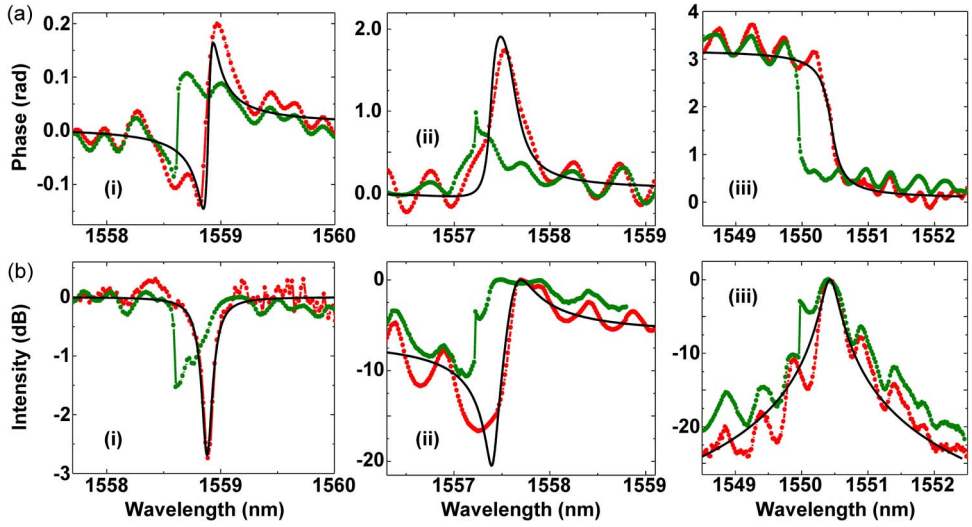

Fig. 4. Measured (a) phase and (b) intensity spectra of (i) open ($t_B^2 = 1$), (ii) partially-blocked ($t_B^2 = 0.1$), and (iii) blocked ($t_B^2 = 0$) structures for two different input powers. Red and green dotted lines are experimental data at low and high input powers, respectively, and black solid lines represent theoretical fits to the low-power, linear case. All the structures have similar cavity Q-factors.

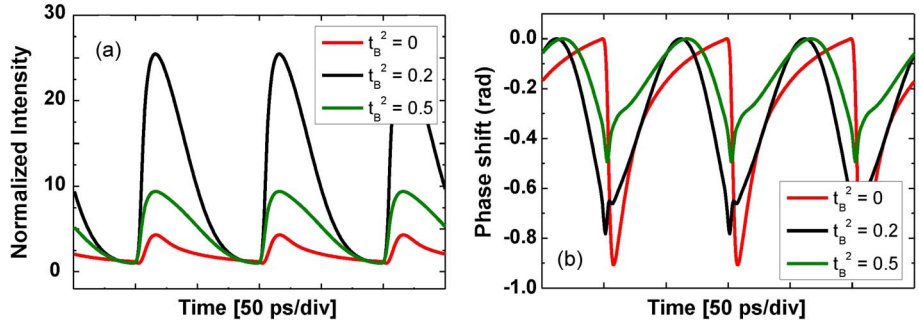

Fig. 5. Calculated transmission and phase dynamics. The transmitted intensity and phase shift is shown versus time for a Lorentzian structure ($t_B = 0$, red curve) and two Fano structures ($t_B = 0.2$, black curve; $t_B = 0.5$, green curve) for 10 GHz all-optical modulation. The three structures have the same Q_t of 4000 and Q_v of 12000. The pump (5 ps pulsewidth) is fixed at the resonant wavelength, and the signal has its wavelength scanned on the blue side of the resonance to achieve the largest intensity modulation contrast.

to give a specific form/value for the chirp-parameter of the switches. However, for the same intensity change, the Fano structure leads to less phase variation than its Lorentzian counterpart, which is the key point here. The ripples in the experimental data are due to residual reflections at the input and output sections of the devices. In Fig. 5 we show examples of simulated transmission and phase dynamics for Fano and Lorentzian structures at 10 GHz. The dynamical results confirm the expectations obtained from the analysis of static spectra. For a large value of the intrinsic quality factor, the transmission contrast is much larger for the Fano than for the Lorentzian structure, while the phase changes are comparable, leading to a much lower chirp-parameter for the Fano structure. Furthermore, by varying the ratio between the total and intrinsic cavity Q-factor, the transmission contrast and the phase change can be adjusted for Fano structures, while being constant for Lorentzian structures. This enables optimization of the performance of Fano structures depending on the specific application.

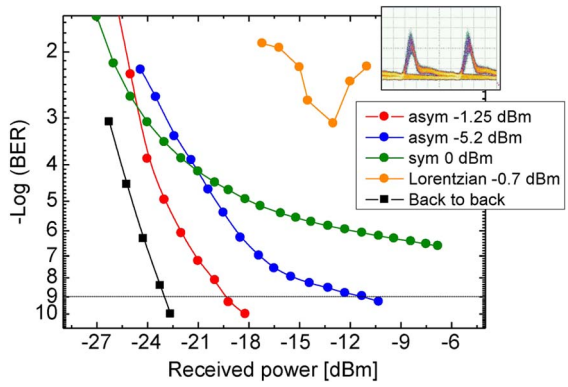

Fig. 6. BER measurements of modulated signal versus received power for different pump energies (colored markers) and back-to-back signal (black markers) at 10 Gbit/s. The red and blue dotted lines correspond to the asymmetric Fano structure operated with a pump power of −1.25 and −5.2 dBm, respectively; the green dotted line corresponds to the symmetric Fano structure operated with a pump power of 0 dBm; the yellow dotted line corresponds to the Lorentzian structure operated with a pump power of −0.7 dBm. (Inset) Measured eye diagram of the asymmetric Fano structure.

3. Improving Switching Performance Using an Asymmetric Fano Structure

Here, we experimentally demonstrate that by breaking the mirror symmetry of a Fano structure, the switching properties can be further improved. Fig. 3(b) shows a fabricated PhC InP membrane employing a smaller H0 nanocavity. Fig. 3(c) shows the spectrum, calculated using a three-dimensional finite-difference time-domain technique, exhibiting an on-off contrast of more than 30 dB within a narrow wavelength range. In the transmission spectrum, a small dip can be seen that is about 5 nm blue-detuned from the main Fano minimum. This dip corresponds to another eigenmode of the H0 cavity. This eigenmode has a relatively high (low) total (intrinsic) Q-factor and does not affect the switching since it is far from the input signals that are located on the red side of the Fano minimum. The mirror symmetry of the structure is broken by displacing the BH by one lattice constant towards port 1. This makes the coupling rate between port 1 and cavity γ_1, differ from the rate between port 2 and cavity γ_2. Recently, a similar structure with broken symmetry was shown to enable non-reciprocal light transmission when combined with an optical nonlinearity [15]. For the present design, FDTD simulations lead to $t_B = 0.24$ and $\gamma_1/\gamma_2 = 2.5$. Transmission from port 1 (2) to port 2 (1) is henceforth denoted as forward (backward).

From simulations we find that compared to the symmetric Fano structure, larger cavity energy and switching contrast are achieved when operating the asymmetric Fano structure in the forward direction, i.e., injecting from port 1. This is due to the switching improvements that can be obtained using asymmetric structures, where larger energy can be coupled into the cavity without sacrificing the Q-factor. This result may seem counter intuitive since the asymmetry of the coupling coefficients can result in a lower transmission; cf. Fig. 1(b). However, the improvement in the nonlinear switching performance compensates for this additional transmission loss.

Next, we experimentally investigate the all-optical switching properties of the structure at bitrates of 10 and 20 Gbit/s. Return-to-zero (RZ) pump pulses (10 ps) are first generated and then modulated in the on-off keying (OOK) format at 10 and 20 Gbit/s with a PRBS of length $2^{31} - 1$. The modulated pump and a CW signal are coupled into the PhC device through port 1. At the output of the device, i.e., port 2, the combined signal is amplified before the modulated signal is separated from the pump using an optical band-pass filter and detected by a receiver. The pump and signal are slightly red-detuned from the Fano resonance maximum and minimum, respectively. Fig. 6 shows the measured BER curves for 10 Gbit/s all-optical modulation. The BER decreases as the pump energy increases due to an enhanced switching contrast. Error-free $(\mathrm{BER} < 10^{-9})$ operation is achieved with a coupled pump power of only −5.2 dBm,

which is several times lower than the result obtained using the H1 cavity with a symmetric configuration (the green dotted line in Fig. 6) [8]. This small energy consumption is mainly ascribed to the asymmetric configuration of the device. Besides, a larger Q/V value of the H0 cavity also acts to reduce the switching energy.

In Fig. 6, a power penalty of 3 dB is seen at 10^{-9} BER for a pump power of –1.25 dBm. Compared with the symmetric Fano and traditional Lorentzian structure (see the yellow dotted line in Fig. 6) [21], we find that patterning effects are significantly suppressed and the energy consumption is reduced in the asymmetric Fano structure, enabling modulation rates higher than the carrier relaxation rate. This speed enhancement originates from the regeneration characteristics of the nonlinear transfer function of the Fano resonance, similarly to the case of nonlinear quantum dot amplifiers [22]. Here the symmetric Fano structure shows lower BER than that of the asymmetric Fano structure below received power of –21 dBm. This might be because the output signal power from the symmetric Fano structure is higher than that of the asymmetric Fano structure. Although the input conditions as well as the receiver configurations for the measurements of the Fano and Lorentzian structures are not identical, they are tuned/adjusted to achieve the best results, and we believe the measured BER curves still reflect the improvement due to the use of Fano effects. Thus, the back-to-back sensitivity is actually even lower for the Lorentzian structure but still an improvement is observed for the Fano structures. As for the Lorentzian structure, the increasing BER values at high received power values are believed to be due to saturation effects in the receiver [21]. The high power penalty induced by the switch forces the receiver to be operated at high optical input power, which saturates the following photodiode.

For 20 Gbit/s operation, we that find the BER increases somewhat, but is still well below the threshold for employing forward error correction (FEC) schemes [12]. Considering backward operation using the same device, we found the performance to be seriously degraded, i.e., 20 Gbit/s modulation cannot be achieved under the same conditions, proving that the advantage of the asymmetric structure originates from the larger coupling from the waveguide into the nanocavity.

4. Conclusion

The intensity and phase response of Lorentzian and Fano cavity-waveguide structures are investigated both experimentally and theoretically. Compared to a traditional Lorentzian structure, the Fano structure is shown to be able to improve the switching contrast and speed without adding any extra phase distortion, leading to a much lower chirp-parameter. Furthermore, by varying the ratio between the total and intrinsic cavity Q-factor, the transmission contrast and the phase change can be adjusted for Fano structures, while being constant for the Lorentzian structure. In addition, we also demonstrate that by breaking the mirror symmetry of the Fano structure, the switching performance can be further improved. Using a simple and ultra-compact InP photonic-crystal Fano structure with broken mirror symmetry, we simultaneously achieve error-free 10 Gbit/s RZ-OOK all-optical modulation with a pump power as low as –5.2 dBm (60 fJ/bit). For 20 Gbit/s operation, a BER three orders lower than the FEC limit is obtained. In both cases, long, telecomgrade, PRBS patterns of length $2^{31} - 1$ were employed. However, the device performance depends on various factors such as cavity Q-factors, transmittivity of the partially transmitting element, material nonlinearities, etc., and it is difficult to state a quantitative improvement of Fano structures with respect to traditional Lorentzian structures. However, the results clearly show that the use of Fano resonances significantly enhances the speed and provides additional design freedom, which may also find other applications, e.g., within sensing.

Acknowledgment

The authors thank C. Peucheret and D. Vukovic for assistance in experiments and helpful discussions.

References

[1] D. A. B. Miller, "Device requirements for optical interconnects to silicon chips," *Proc. IEEE*, vol. 97, no. 7, pp. 1166–1185, Jul. 2009.

[2] D. M. Beggs, T. P. White, L. O'Faolain, and T. F. Krauss, "Ultracompact and low-power optical switch based on silicon photonic crystals," *Opt. Lett.*, vol. 33, no. 2, pp. 147–149, 2008.

[3] C. Husko *et al.*, "Ultrafast all-optical modulation in GaAs photonic crystal cavities," *Appl. Phys. Lett.*, vol. 94, no. 2, 2009, Art. ID 021111.

[4] Q. Xu, B. Schmidt, S. Pradhan, and M. Lipson, "Micrometre-scale silicon electro-optic modulator," *Nature*, vol. 435, no. 7040, pp. 325–327, May 2005.

[5] K. Nozaki *et al.*, "Sub-femtojoule all-optical switching using a photonic-crystal nanocavity," *Nature Photon.*, vol. 4, pp. 477–483, 2010.

[6] A. Bazin *et al.*, "Ultrafast all-optical switching and error-free 10 Gbit/s wavelength conversion in hybrid InP-silicon on insulator nanocavities using surface quantum wells," *Appl. Phys. Lett.*, vol. 104, no. 1, 2014, Art. ID 011102.

[7] U. Fano, "Effects of configuration interaction on intensities and phase shifts," *Phys. Rev.*, vol. 124, no. 6, pp. 1866–1878, Dec. 1961.

[8] Y. Yu *et al.*, "Fano resonance control in a photonic crystal structure and its application to ultrafast switching," *Appl. Phys. Lett.*, vol. 105, 2014, Art. ID 061117.

[9] Y. Yu *et al.*, "Switching characteristics of an InP photonic crystal nanocavity: Experiment and theory," *Opt. Exp.*, vol. 21, no. 25, pp. 31047–31061, 2013.

[10] M. Heuck *et al.*, "Heterodyne pump probe measurements of nonlinear dynamics in an indium phosphide photonic crystal cavity," *Appl. Phys. Lett.*, vol. 103, no. 18, 2013, Art. ID 181120.

[11] Y. Yu, H. Hu, L. K. Oxenlowe, K. Yvind, and J. Mork, "Ultrafast low-energy all-optical switching using a photonic-crystal asymmetric Fano structure," in *Proc. IEEE Int. Conf. Photon. Switch.*, 2015, pp. 94–96.

[12] Y. Yu, H. Hu, L. K. Oxenlowe, K. Yvind, and J. Mork, "Ultrafast all-optical modulation using a photonic-crystal Fano structure with broken symmetry," *Opt. Lett.*, vol. 40, pp. 2357–2360, 2015.

[13] M. Heuck, P. T. Kristensen, Y. Elesin, and J. Mork, "Improved switching using Fano resonances in photonic crystal structures," *Opt. Lett.*, vol. 38, pp. 2466–2468, 2013.

[14] S. H. Fan, "Sharp asymmetric line shapes in side-coupled waveguide-cavity systems," *Appl. Phys. Lett.*, vol. 80, pp. 908–910, 2002.

[15] Y. Yu *et al.*, "Nonreciprocal transmission in a nonlinear photonic-crystal Fano structure with broken symmetry," *Laser Photon. Rev.*, vol. 9, no. 2, pp. 241–247, Mar. 2015.

[16] S. H. Fan, W. Suh, and J. D. Joannopoulos, "Temporal coupled-mode theory for the Fano resonance in optical resonators," *J. Opt. Soc. Amer. A, Opt. Image Sci.*, vol. 20, no. 3, pp. 569–572, 2003.

[17] Q. V. Tran, S. Combrie, P. Colman, and A. D. Rossi, "Photonic crystal membrane waveguides with low insertion losses," *Appl. Phys. Lett.*, vol. 95, no. 6, 2009, Art. ID 061105.

[18] Y. Yu *et al.*, "Experimental demonstration of a four-port photonic crystal cross-waveguide structure," *Appl. Phys. Lett.*, vol. 101, no. 25, 2012, Art. ID 251113.

[19] F. Koyama and K. Ida, "Frequency chirping in external modulators," *J. Lightw. Technol.*, vol. 6, no. 1, pp. 87–93, Jan. 1988.

[20] W. Q. Xue and J. Mork, "Tunable true-time delay of a microwave photonic signal realized by cross gain modulation in a semiconductor waveguide," *Appl. Phys. Lett.*, vol. 99, no. 23, 2011, Art. ID 231102.

[21] D. Vukovic *et al.*, "Wavelength conversion of a 9.35 Gb/s RZ OOK signal in an InP photonic crystal nanocavity," *IEEE Photon. Technol. Lett.*, vol. 26, no. 3, pp. 257–260, Feb. 2014.

[22] A. V. Uskov, T. W. Berg, and J. Mork, "Theory of pulse-train amplification without patterning effects in quantum-dot semiconductor optical amplifiers," *IEEE J. Quantum Electron.*, vol. 40, no. 3, pp. 306–320, Mar. 2004.